

Chemical analysis of Antarctic regolith and lunar regolith simulant as prospective substrates for experiments with plants

Pavel Coufalík^{1*}, Hector-Andreas Stavrakakis², Dimitra Argyrou²

¹*Institute of Analytical Chemistry of the Czech Academy of Sciences, Veveří 97, 602 00 Brno, Czech Republic*

²*National Technical University of Athens, School of Mining and Metallurgical Engineering, Department of Geological Sciences, Athens, Greece*

Abstract

This study investigates the viability of Antarctic regolith and a lunar regolith simulant as prospective substrates for plant growth under extreme conditions. The study is focused on chemical composition of both substrates with a special respect to heavy metals. The Antarctic regolith samples were collected from James Ross Island, while lunar regolith simulant was developed in order to access the mobility and bioavailability of trace metals in these substrates, using a modified BCR (Community Bureau of Reference) sequential extraction procedure. Cadmium (Cd) and zinc (Zn) are among the significant mobile fractions, indicating their possible effects on the germination and growth of plants. Additionally, preliminary results from the study of the regolith samples at the area of Berry Hill mesa are presented, as well as the chemical and mineralogical affinity of the Antarctic regolith and the produced lunar simulant to lunar regolith. The findings suggest that such Antarctic environment can be used in astrobiological studies and future lunar habitation efforts to sustainably cultivate plants and perform other biological experiments on these extraterrestrial surfaces. This is an important concept in light of active programs like Artemis and Gateway.

Key words: lunar regolith simulant, heavy metal, BCR extraction, Antarctica, James Ross Island, ISRU, agriculture

DOI: 10.5817/CPR2024-2-15

Introduction

Several studies have investigated the ability of plant growth in space conditions for assessing the prospects of life survivability, but also for the current focus of in situ resource utilization (ISRU) purposes (Hossner et al. 1991, Ming and Henninger 1994, Eichler et al. 2021, Fackrell et al. 2021, Paul et al. 2022). Such work has

Received December 13, 2024, accepted January 20, 2025.

*Corresponding author: P. Coufalík <coufalik@iach.cz>

Acknowledgements: The authors thank for the support provided by the projects VAN22, VAN23 (MŠMT), Czech Antarctic infrastructure (CARI), CAERPIN-MU Brno, and the EEL laboratory (UEB MU Brno) for sample collection at the James Ross Island. The work of PC was supported by the Czech Science Foundation under grant No. 24-10051S.

been accomplished by utilising regolith retrieved from the moon through the Apollo missions or via regolith analogue and simulant materials (Mortley *et al.* 2000, Eichler *et al.* 2021, Fackrell *et al.* 2021, Duri *et al.* 2022, Paul *et al.* 2022). Though Martian conditions have been given increased interest in the past, the lunar environment is equally important to be investigated. This is true especially in the present era which plan for constant human presence in the lunar environment via the Artemis and Getway programs.

A mobile proportion of metals released from the regolith is decisive for ecotoxicity, not their total content, which also includes fractions bound in silicates. The mobile fraction includes the chemical species of metals, which are able to release into the liquid phase under certain conditions. Thus, the forms of metals releasable in water, weakly bound metal complexes, or even the fraction bound to carbonates, are often referred to the mobile fraction (Hlavay *et al.* 2004).

The selective and sequential extraction procedures have been developed since the 1980's to assess the mobility/bioavailability of metals in sediments and soils (Hlavay *et al.* 2004). Most often, they divide the total metal content into fractions according to their binding to matrix components. Generally, the main parameters affecting the extraction yield are the type

and concentration of the extractant, the phase ratio, and the extraction time. The fundamental problem of these procedures was mainly the inconsistency of the analytical procedures, which makes it impossible to compare the achieved results. The European Commission (EU) introduced the use of optimized sequential extraction proposed by the Community Bureau of Reference protocol (BCR) (Arain *et al.* 2008, Hlavay *et al.* 2004, Kubová *et al.* 2004, Rauret *et al.* 2000, Ure *et al.* 1993), which provides sufficiently robust and comparable results suitable for the validation of certified reference materials.

The aim of this study was to determine the mobile fraction of metals in lunar regolith simulant and Antarctic regolith, which were selected as model substrates for monitoring the inhibition of plant germination under extreme conditions. Furthermore, preliminary results of the regolith samples collected from the area surrounding the Berry Hill mesa on James Ross Island (Antarctica) are presented from the ongoing geological analysis performed at the National Technical University of Athens (NTUA), Greece. The study also aimed to the evaluation of an Antarctic regolith, its suitability and advantage for future studies with plants grown in substrates mimicking the surface structures of extraterrestrial planets and their moons.

Material and Methods

Samples and certified reference materials

Lunar regolith simulant

The lunar regolith simulant was developed at the National Technical University of Athens (NTUA), Greece. The NTUA group has developed and provided to the scientific community a range of lunar regolith and dust simulants, as well Martian

simulants (Stavarakakis *et al.* 2022, Argyrou *et al.* 2024). The aim of the group has been to provide a range of simulants based on surface sample datasets that are representative of the varied characteristics and lithology of the respective environments.

For achieving this goal, the team has focused on utilising and optimising a multi mineral-rock approach during the simulant development process (Stavarakakis et al. 2022, Argyrou et al. 2024), while developing new technologies, methodologies and frameworks (Chatzitheodoridis et al. 2024). The Lunar regolith simulant utilised in this study was part of the fifth batch (“L5”) of produced Lunar simulants by the team, which was developed based on the Apollo 15 15260 sample (Fig. 1). The Apollo 15260 sample was collected at a depth of approximately 25cm from the lunar surface, allowing it to be partially shielded by the erosion effects of top soil (*i.e.* cosmic radiation and micrometeorites), leading to a more representative sample candidate of material likely to be used in ISRU pur-

poses. The “L5” Lunar regolith simulant batch includes a suite of igneous rocks ranging from mafic basaltic samples to felsic dacite samples, collected during field trips to the volcanic Santorini Island, Greece, as well as commercial (*e.g.* Dr. F. Krantz Rheinisches Mineralien-Kontor GmbH & Co, Germany) and other sources (*e.g.* laboratory inventory), providing the following components list: basalt, dunite, hematite, anhydrite, labradorite, apatite, ilmenite. The mineral and rock components utilised for the synthesis of the simulants had firstly been crushed and grounded to a grain fraction of under 1 mm before fine tuning to the targeted chemical, mineralogical and grain size distribution characteristics, of under 250µm.

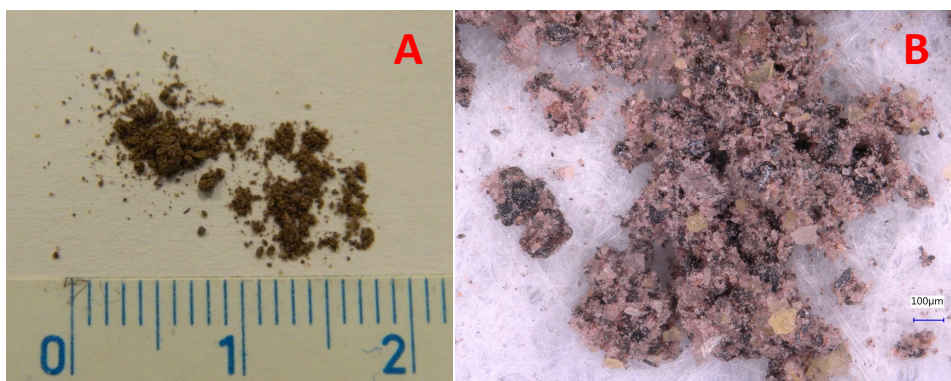


Fig. 1. View and texture of the “L5” Lunar regolith simulant produced at National Technical University of Athens (NTUA), Greece. In picture B, close up view allowing for better understanding of the simulant’s grain size distribution.

Antarctic regolith

Antarctic regolith was collected at the James Ross Island (Antarctica), from the foothill of Northern slopes of Berry Hill mesa (57° 50′ 19″ W, 63° 48′ 54″ S) at the Ulu Peninsula (Fig. 2). The geologic background of the surrounding outcrops of the Ulu Peninsula and additional information regarding the broader geomorphology, petrology, and geochemical composition of the area outcrops can be found in a

number of other works, though the area is still under investigation (Smellie et al. 2006, 2008, 2013; Košler et al. 2009, Mlčoch et al. 2013, 2018; Altunkaynak et al. 2018). The collected bulk sampled regolith can be seen in Fig. 3. On site and initial laboratory observation suggest that the sampled regolith is dominated by fragments of hyaloclastic breccias.

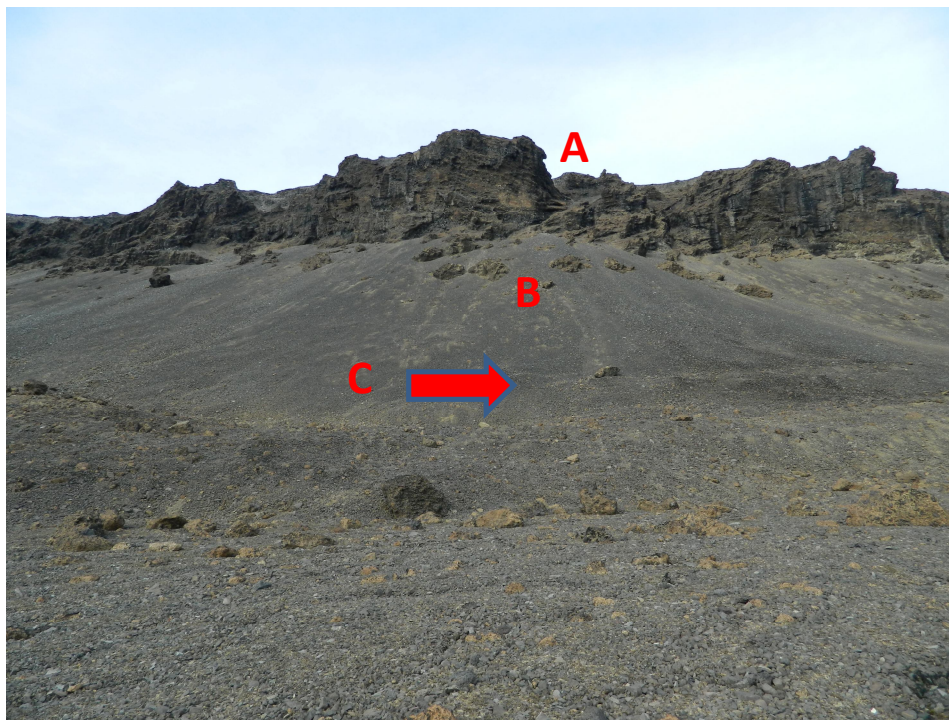


Fig. 2. Northern slopes of Berry Hill mesa showing A) Volcanic rock walls of the top B) Rock fragments forming a rubble slope C) Site of regolith collection on the foothill.



Fig. 3. Collected Antarctic regolith sample. In the picture A, the regolith can be seen as it was sampled. In the picture B, a material distribution is shown starting from the left of the picture with fine silty material up to mm thick sand grains in the middle and pebble sized rocks on the right side.

Standard soil materials

In addition to the described regolith samples, following certified reference materials (CRMs) were also used to verify the accuracy of the determination of metals:

Montana II Soil 2711a (NIST, USA), and BCR-483 Soil (IRMM, Belgium). The main reason for using these CRMs was to verify an extraction procedure.

Analytical procedures

The chemical and mineralogical composition of Antarctic regolith was determined via SEM-EDS and XRD analysis respectively. The provided "L5" Lunar regolith simulant underwent only chemical compositional analysis via SEM-EDS, as the mineralogical makeup of the simulant was known because known mineralogically components have been used.

For the SEM-EDS analysis, the finer components of Antarctic regolith sample were crushed into fine particulate and homogenized in order to attain a bulk mean composition of this regolith fraction, in an agate mortar and an agate pestle, before being pressed in custom-made disk-shaped tablet sample holders. The "L5" Lunar simulant was directly pressed into the custom-made sample holder since it was already homogenized as fine particulate material. The SEM-EDS analyses were made in Low Vacuum (30 Pa) setting at 20 kV and similar $\times 100$ zoom setting, providing approximately a $950\ \mu\text{m}$ by $1250\ \mu\text{m}$ scanned area. Then after, the samples were scanned for 300 seconds for bulk chemistry in random locations across the disk tablet and the average value of those was calculated to minimised local enrichment bias. In the case of the Antarctic regolith, 7 different measurements were made, while in the case of the simulant, 3 random locations were chosen as it was developed from already known chemically components.

For the XRD analysis the processed Antarctic regolith was further refined to a fraction smaller than $50\ \mu\text{m}$, before being pressed in the special XRD sample holder.

Trace metal analysis of the samples was performed in a clean laboratory with HEPA filters, in a clean bench. The grain fraction $< 2\ \text{mm}$ was sieved for the analysis of regolith from JRI. The weight of $0.5\ \text{g}$ of each sample was used for the analysis for any procedure and repetition. Two liquid extractions were performed to simulate the release of the mobile fraction of metals. The digestion in concentrated HNO_3 was also carried out to determine the total available amount of metals, hereinafter referred to as the total content.

To evaluate the mobile fraction of metals in the regolith, the first step of BCR sequential extraction (European Commission, EU) was performed. The procedure included the extraction on a shaker (GFL 3018, Germany) in $0.11\ \text{mol/L}$ CH_3COOH (Suprapur, 96%, Merck, Germany) in a ratio of $0.5\ \text{g}$ of sample per $20\ \text{mL}$ of solution at laboratory temperature (22°C) for 16 h (Arain et al. 2008, Rauret et al. 2000). Extraction in deionized water was carried out under the same conditions for the purpose of comparing extraction yields. Subsequently, the extracts were centrifuged (Centrifuge 5804R, Eppendorf AG, Germany) at $9\ 000\ \text{g}$ for 10 min., and collected into HDPE scintillation vials (Kartell, Italy).

The total metal contents were determined after digestion in $5\ \text{mL}$ of subboiling HNO_3 using an UltraWAVE microwave mineralizer (Milestone, Italy) at 250°C for 20 min. The digests were then diluted with deionized water and stored in scintillation vials until the analysis.

The determination of metals in both extracts and digests was carried out by means of electrothermal atomic absorption spectrometry (ETAAS) using an Analyst 600 (PerkinElmer, USA) under optimized conditions (Tables 1, 2). A pre-mixed matrix modifier ($\text{Mg}(\text{NO}_3)_2 \cdot 6\text{H}_2\text{O}/\text{NH}_4\text{H}_2\text{PO}_4$ Suprapur, 99.99%, Pb, Cd ≤ 0.005 mg/kg, Merck, Germany) was used for the deter-

mination of Cd and Pb. Three parallel analyzes were performed for each sample, extraction and digestion. Appropriate methodical blanks were processed and analyzed together with the samples. The Cd, Cr, Cu, Ni, Pb, and Zn standards for AAS (1000 ± 4 mg/L, Sigma-Aldrich, Switzerland) were used for calibration purposes using the method of standard additions.

	Cd	Cr	Cu	Ni	Pb	Zn
Wavelength (nm)	228.8	357.9	324.8	232.0	283.3	213.9
Slit (nm)	0.7	0.7	0.7	0.2	0.7	0.7
Source ^a /Current (mA)	HCL/4	HCL/25	HCL/15	HCL/25	HCL/10	EDL240

Table 1. Spectral parameters for determination of metals by means of ETAAS.

Note: ^aHCL/EDL – Hollow Cathode Lamp / Electrodeless Discharge Lamp.

Step	Temperature (°C) / Ramp Time (°C/s) / Hold Time (s)					
	Cd	Cr	Cu	Ni	Pb	Zn^a
Drying 1	110/1/20	110/1/20	110/1/20	110/1/20	110/1/20	110/1/20
Drying 2	130/15/30	130/15/30	130/15/30	130/15/30	130/15/30	130/15/30
Pyrolysis	500/20/20	1000/10/20	900/10/20	1100/10/20	800/20/20	500/20/20
Atomization	1600/0/3	2300/0/5	2100/0/5	2300/0/5	1600/0/3	1800/0/3
Cleaning	2450/1/2	2600/1/2	2450/1/2	2600/1/2	2450/1/2	2600/1/2

Table 2. Temperature programs for determination of metals by means of ETAAS.

Note: ^aInternal Ar flow 250 mL min⁻¹.

Results and Discussion

SEM-EDS

The simulants developed at the National Technical University of Athens (NTUA), are based on semi-autonomous process that matches the chemistry and mineralogy of the components utilised to the target data, based on a Figure of Merit (FOM) system (Schrader *et al.* 2009). Thus,

the highest possible compositional match can be calculated for the simulant based on the available material components. This process provides an estimated “Theoretical” Figure of Merit (FOM) that is then compared with the results (Table 3).

	Duncan 75	L5 Estimated	L5 Measured	FOM L5 Estimated to Duncan 75	FOM L5 Measured to Duncan 75
Na₂O	0.39	2.14	2.51	0.39	0.39
MgO	10.77	10.41	10.95	10.41	10.77
Al₂O₃	16.49	15.83	16.12	15.83	16.12
SiO₂	46.61	47.13	44.92	46.61	44.92
P₂O₅	0.22	0.28	0.25	0.22	0.22
SO₃	0.08	0.36	0.39	0.08	0.08
Cl	0.00	0.00	0.00	0.00	0.00
K₂O	0.19	0.38	0.38	0.19	0.19
CaO	11.21	9.74	9.83	9.74	9.83
TiO₂	1.51	1.54	0.88	1.51	0.88
Cr₂O₃	0.00	0.10	0.29	0.00	0.00
MnO	0.16	0.05	0.07	0.05	0.07
FeO (Fe₂O₃)*	12.35	12.02	13.41	12.02	12.35
SUM	100.00	100.00	100.00	97.08	95.83

Table 3. The Apollo 15260 sample analysis (Duncan et al. 1975) compared to the estimated and measured composition, together with chemical resemblance Figure of Merit (FOM value).

Note: The values were normalised for accurate FOM calculations. *All the Fe is reported as FeO.

The provided results show that the developed simulant has a FOM score of 95.83, suggesting a very high chemical resemblance with the target lunar regolith sample composition. It is worth noting that a significant deviation on the alkali content exists. The required low values are extremely difficult to fully simulate and adjust with terrestrial source materials, as the conditions of the lunar surface cause a significant depletion of those elements. However, despite Apollo and Chang'e missions data suggest that sodium levels are below 1 wt.% globally, orbital spectral analysis provides a Sodium average abundance of 1.33 wt% (Narendranath et al. 2022). In either case, a significant portion of the original alkali content of the Moon has been suggested to occur due to evaporation losses during its initial formation

process (Steenstra et al. 2018). Additionally, the grain size distribution as was calculated via SEM-EDS and photographic grain analysis suggests that the simulant has the majority of its grains at less than 250 μm and a median at less than 125 μm which is well into accordance and good accuracy of the 15260-target grain distribution.

The data reported on the bulk fine portion of the Antarctic regolith sample from the northeastern area of the Berry Hill mesa can be found in Table 4. The data suggest that the sample should be classified (based on the TAS classification, Le Maitre et al. 2002) as Basaltic andesite, due to its intermediate felsic content. However, the results have produced a number of questions that need to be resolved by the ongoing investigation. Initial-

ly, disparities can be identified when the regolith chemistry data are compared to the data from rock samples from the top of Berry Hill mesa (JR59, JR61A, JR61B) and similar hyaloclastic breccias samples (JR-104 and JR-109) of the Ulu peninsula, *see* Table 4, from the works of Košler *et al.* (2009), and Altunkaynak *et al.* (2018)

respectively, which are placed as high alkali Basalts based on the TAS classification. Furthermore, from the 6 target areas analysed, only half provided phosphor (P) presence in the bulk fine Antarctic regolith (Table 4), while in all other cases phosphor (P) presence had been reported (Table 5).

Site of Interest	1	2	3	4	5	6	Average	Fom Duncan to Disk Average	Fom L5 to Disk Average
Na₂O	2.81	2.77	2.76	1.81	2.88	3.18	2.69	0.39	2.51
MgO	5.53	5.23	6.19	15.06	6.25	6.59	7.46	7.46	7.46
Al₂O₃	17.37	18.66	19.54	16.19	20.13	20.36	18.66	16.49	16.12
SiO₂	54.23	56.59	55.69	50.73	56.40	59.02	55.30	46.61	44.92
P₂O₅	0.49	0.00	0.72	0.00	0.76	0.00	0.33	0.22	0.25
SO₃	0.00	0.00	0.00	0.00	0.00	0.00	0.00	0.00	0.00
Cl	0.00	0.00	0.00	0.00	0.00	0.00	0.00	0.00	0.00
K₂O	1.63	1.59	1.67	0.80	1.43	1.32	1.40	0.19	0.38
CaO	5.07	4.34	3.91	4.03	3.97	3.28	4.09	4.09	4.09
TiO₂	1.95	1.62	1.54	0.00	1.39	1.33	1.56	1.51	0.88
Cr₂O₃	0.00	0.00	0.00	0.00	0.00	0.00	0.00	0.00	0.00
MnO	0.00	0.00	0.00	0.00	0.00	0.00	0.00	0.00	0.00
FeO (Fe₂O₃) *	10.90	9.20	7.99	11.39	6.79	4.93	8.51	8.51	8.51
SUM	99.98	100.00	100.01	100.01	100.00	100.01	100.00	85.48	85.13

Table 4. Individual measurements on the disk tablet from the bulk fine portion of the Antarctic regolith sample, and Figure of Merit comparison data to the Lunar regolith sample and the “L5” Lunar regolith simulant. *Note:* All analyses are recalculated to 100%. *All the Fe is reported as FeO.

The associated Figure of Merit scores compared to the Lunar surface (Apollo 15260 sample) is 85.48, and the produced “L5” Lunar regolith simulant has a score of 85.13. The Figure of Merit (FOM) scores, together with the TAS classification indicate a medium material correlation in chemical composition. On the scope of mineralogical similarities, the Antarctic regolith sample, due to its hyaloclastic na-

ture, is high glass content which coincides with the significant glass portion contents identified in the lunar regolith. Additionally, the XRD analysis has verified very high glass content, while number of minerals expected to be found in the lunar regolith were identified. Furthermore, the TAS placement and the chemical affinity of the sampled location from Table 5 to the Lunar regolith target (Apollo 15260) have

with Figure of Merit score at around 95 suggesting that the materials from the area can be considered of high quality. Additionally, the identification of secondary clay minerals via XRD coincide with expected alterations occurring from the high-

ly active water-rock interaction environment present in the area, *e.g.* glacial environment, and suggest that future work should be done investigating possible correlations with the Martian surface environments.

Samples	Duncan 75	L5 Measured	JR59 ¹	JR61A ¹	JR61B ¹	JR-104 ²	JR-109 ²	Average of 6
Na ₂ O	0.39	2.51	3.50	3.60	3.82	3.55	3.94	2.69
MgO	10.77	10.95	9.12	8.64	8.58	9.66	9.46	7.46
Al ₂ O ₃	16.49	16.12	15.40	15.69	15.59	15.44	15.49	18.66
SiO ₂	46.61	44.92	49.36	49.16	49.17	47.61	47.67	55.30
P ₂ O ₅	0.22	0.25	0.42	0.41	0.41	0.55	0.62	0.33
SO ₃	0.08	0.39	n/a ³	n/a ³	n/a ³	n/a ³	n/a ³	0.00
Cl	0.00	0.00	n/a ³	n/a ³	n/a ³	n/a ³	n/a ³	0.00
K ₂ O	0.19	0.38	1.24	1.39	1.27	1.38	1.52	1.40
CaO	11.21	9.83	7.48	7.85	7.82	7.83	7.50	4.09
TiO ₂	1.51	0.88	1.55	1.49	1.53	1.75	1.74	1.56
Cr ₂ O ₃	0.00	0.29	0.04	0.04	0.04	0.04	0.03	0.00
MnO	0.16	0.07	0.18	0.18	0.18	0.16	0.16	0.00
FeO (Fe ₂ O ₃)*	12.35	13.41	11.70	11.55	11.59	12.03	11.87	8.51
Total Percentage	100.00	100.00	100.00	100.00	100.00	100.00	100.00	100.00

Table 5. Comparison with data from sampling locations of previous works performed at the Ulu peninsula of James Ross Island. *Note:* All the values were normalised to 100. ¹Košler et al. 2009, ²Altunkaynak et al. 2018, ³The elements were not measured at the respective papers, *All the Fe is reported as FeO.

Berry Hills Fine

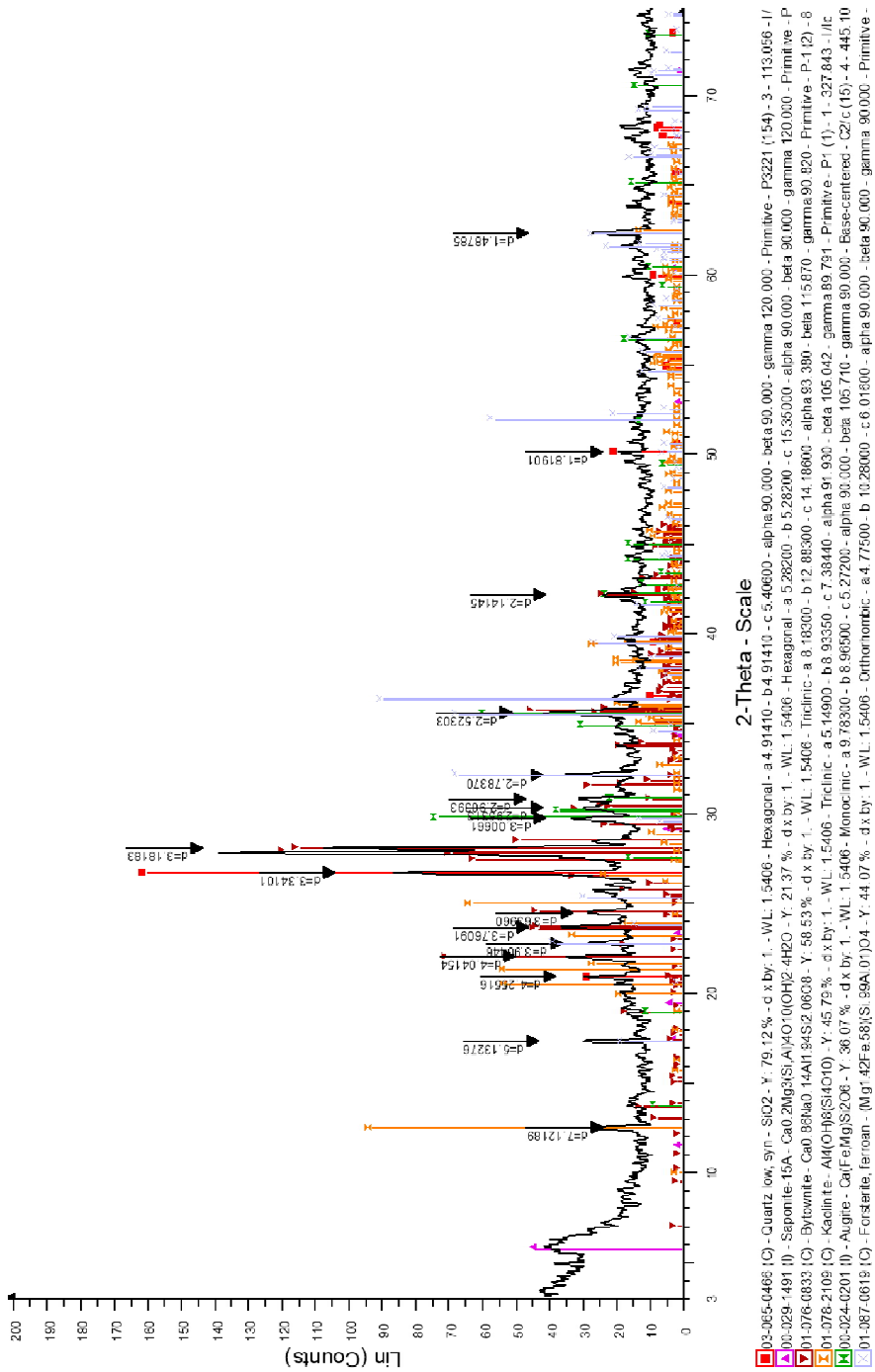


Fig. 4. XRD diagram of the bulk fine regolith sample with identified primary and secondary minerals.

Trace metals analysis

The Cd, Cr, Cu, Ni, Pb, and Zn are the metals selected at the beginning of the BCR program to harmonize the methodology of metal speciation in sediments due to their toxicity in the environment (Ure et al. 1993).

The mobile fractions and total metal contents of these metals in samples and CRMs are summarized in Table 6. Limits of detection (LOD) and limits of quantification (LOQ) are calculated as three times and ten times the standard deviation of me-

thodical blanks, respectively. Determined total metal contents (in HNO₃ digests) in the samples do not include the proportion of metals bound in the silicates. Also, it is not a pseudo-total metal content (Hlavay et al. 2004), which is referred to the digestion in the aqua regia. (The aqua regia dissolves metals from otherwise insoluble sulfides; and so, it is not suitable for assessing the potentially mobilizable proportion of metals.)

	Regolith JRI	Regolith 15260GR, L5	Montana II Soil 2711	BCR483 Soil	LOD	LOQ
Cd (H ₂ O)	<LOD	<LOD	0.2±0.0008	0.211±0.0003	0.0002	0.0008
Cd (HAc)	0.0101 ±0.0004	0.0130 ±0.0003	33.2 ±0.3	9.3 ±0.2	0.0001	0.0002
Cd (HNO ₃)	0.0522 ±0.0005	0.0382 ±0.0003	53.8 ±0.1	32 ±2	0.0001	0.0004
Cr (H ₂ O)	0.060±0.005	0.040±0.001	0.025±0.002	4.3±0.1	0.003	0.011
Cr (HAc)	0.292±0.011	3.00±0.04	0.13±0.002	12.7±0.1	0.001	0.004
Cr (HNO ₃)	30.1±1.2	86±2	20.3±0.1	3204±42	0.003	0.009
Cu (H ₂ O)	0.115±0.007	0.034±0.001	1.74±0.04	7.21±0.07	0.001	0.003
Cu (HAc)	0.167±0.009	0.374±0.009	5.2±0.1	23.4±0.2	0.016	0.053
Cu (HNO ₃)	15.6±0.8	13.0±0.2	125±0.2	332±12	0.014	0.046
Ni (H ₂ O)	0.082±0.014	0.279±0.009	0.071±0.001	2.78±0.07	0.002	0.006
Ni (HAc)	0.623±0.031	19.7±0.7	1.8±0.1	18.3±0.1	0.008	0.025
Ni (HNO ₃)	32.9±0.5	413±10	19.9±0.2	53.6±0.4	0.013	0.045
Pb (H ₂ O)	0.008±0.001	0.006±0.001	2.56±0.07	0.80±0.02	0.002	0.006
Pb (HAc)	<LOD	0.014±0.001	292±1	0.622±0.014	0.003	0.011
Pb (HNO ₃)	4.0±0.2	1.20±0.02	1436±29	503±5	0.002	0.008
Zn (H ₂ O)	0.238±0.027	<LOD	0.665±0.004	14.3±0.6	0.008	0.028
Zn (HAc)	1.37±0.04	11.5±0.3	54.6±0.7	431±8	0.008	0.028
Zn (HNO ₃)	43.9±0.5	21.0±0.2	377±2	1042±2	0.030	0.098

Table 6. Metal contents in extracts and digests of samples and certified reference materials (mg/kg).

The certified and reported metal contents in the certified materials used are listed in Table 7. The determined content of some metals in HNO₃ digests of Montana II Soil 2711 may be lower than certified (Table 7) because a decomposi-

tion in HF was used for the certification. The determined contents in BCR483 Soil corresponded with the certified ones (in the aqua regia) for Cd, Cr, and Pb; others were also lower. In uncontaminated sediments and soils, trace metals exist mostly

bound to primary minerals or bound in silicates, and are released mainly by weathering processes (Hlavay *et al.* 2004).

An acetic acid in the performed extraction mainly extracted the metals associated with calcium carbonate, kaolinite, potassium-feldspar, and ferrihydrite (Hlavay *et al.* 2004). The results of BCR483 extraction in acetic acid (Table 6) were in agreement with the certified contents of the first step of the BCR extraction for Cd, Cr, Ni,

Pb, and Zn (Table 7). The Cd and Zn in regolith samples proved a relatively high mobility according to the extractable fraction (percentage of the total content) in dilute acetic acid (Table 6). A release of metals from regoliths in deionized water tended to be lower than in the first step of BCR extraction. However, the extraction yield in deionized water may depend on the pH of the sample (Arain *et al.* 2008).

	Montana II Soil 2711	BCR483 Soil
Cd (HAc)	-	10.0±0.77
Cd (Total)	54.1±0.5	36.4±2.8
Cr (HAc)	-	9.4±3.5
Cr (Total)	52.3±2.9	3392±484
Cu (HAc)	5±0.04 ^a	16.8±1.5
Cu (Total)	140±2	362±12
Ni (HAc)	-	17.9±2.0
Ni (Total)	21.7±0.7	63.8±7.7
Pb (HAc)	279±1 ^a	0.756±0.70
Pb (Total)	1400±10	501±47
Zn (HAc)	37±0.2 ^a	441±39
Zn (Total)	414±11	987±37

Table 7. Certified and reported^d contents of metals in CRMs (mg/kg). *Note:* ^aKubová *et al.* (2004).

Concluding, via the analytical techniques used in this study (SEM-EDS, XRD & BCR), the characteristics and parameters of the Antarctic regolith and “L5” Lunar regolith simulant were established. With regard to the low absolute amount of observed metals in the mobile fraction, the germination of seeds and cultivation experiments can be performed using these materials in the future astrobiological plant studies. The “L5” Lunar regolith simulant as reported can be considered a good mineralogical match, while also achieving a very good chemical representation with a FOM score of 95.83 and having accurate grain size distribution. The

preliminary results from the Antarctic regolith suggest that the sampled location has a FOM 85.48 to the lunar regolith (15260, Apollo mission) while also having mineralogical match similar to that of the broader lunar environment. Thus, both materials can be considered as good candidate simulants and analogue materials for ISRU and agriculture work simulating the lunar regolith. However, further work is required on the sampled material around Berry Hill mesa to interpret the present data, while also to expand and investigate on the capacity the similarity of the location to the lunar, and possibly Martian, surface.

References

- ALTUNKAYNAK, S., ALDANMAZ, E., GÜRASLAN, I., CALISKANOGLU, A. Z., ÜNAL, A. and NÝVLT, D. (2018): Lithostratigraphy and petrology of Lachman Crags and Cape Lachman lava-fed deltas, Ulu Peninsula, James Ross Island, north-eastern Antarctic Peninsula: Preliminary results. *Czech Polar Reports*, 8: 60-83. doi: 10.5817/CPR2018-1-5
- ARAIN, M. B., KAZI, T. G., JAMALI, M. K., AFRIDI, H. I., JALBANI, N., SARFRAZ, R. A., BAIG, J. A., KANDHRO, G. A. and MEMON, M. A. (2008): Time-saving modified BCR sequential extraction procedure for the fraction of Cd, Cr, Cu, Ni, Pb and Zn in sediment samples of a polluted lake. *Journal of Hazardous Materials*, 160(2–3), 235-239. doi: 10.1016/j.jhazmat.2008.02.108
- ARGYROU, D., STAVRAKAKIS, H.-A. and CHATZITHEODORIDIS, E. (2024): Synthesizing Mars: Advancements in simulant lithology for astrobiological and ISRU studies. EGU General Assembly 2024, Vienna, Austria, 14–19 April 2024, EGU24-12957. doi: 10.5194/egusphere-egu24-12957
- DUNCAN, A. R., SHER, M. K., ABRAHAM, Y. C., ERLANK, A. J., WILLIS, J. P. and AHRENS, L. (1975): Interpretation of compositional variability of Apollo 15 soils. *Proceedings 6th Lunar Science Conference*, pp. 2309–2320.
- DURI, L. G., CAPORALE, A. G., ROUPHAEL, Y., VINGIANI, S., PALLADINO, M., DE PASCALE, S. and ADAMO, P. (2022): The potential for lunar and Martian regolith simulants to sustain plant growth: A multidisciplinary overview. *Frontiers in Astronomy and Space Sciences*, 8: 747821. doi: 10.3389/fspas.2022.747821
- EICHLER, A., HADLAND, N., PICKETT, D. E., MASAITIS, D., HANDY, D. C., PEREZ, A., BATCHELDOR, D., WHEELER, B. A. and PALMER, A. G. (2021): Challenging the agricultural viability of Martian regolith simulants. *Icarus*, 354: 114022. doi: 10.1016/j.icarus.2020.114022
- FACKRELL, L. E., SCHROEDER, P. A., THOMPSON, A., STOCKSTILL-CAHILL, K. and HIBBITTS, C. A. (2021): Development of Martian regolith and bedrock simulants: Potential and limitations of Martian regolith as an in-situ resource. *Icarus*, 354: 114055. doi: 10.1016/j.icarus.2021.114055
- CHATZITHEODORIDIS, E., GEORGIU, C. D., FERUS, M., KALAITZOPOULOU, E., STAVRAKAKIS, H.-A., MARKOPOULOS, I. and HOLYNSKA, M. (2024): Sensing technologies for the challenging lunar environment. *Advances in Space Research*, 74(7): 3407-3436. doi: 10.1016/j.asr.2024.07.017
- HLAVAY, J., PROHASKA, T., WEISZ, M., WENZEL, W. W. and STINGEDER, G. J. (2004): Determination of trace elements bound to soils and sediment fractions (IUPAC Technical Report). *Pure and Applied Chemistry*, 76(2): 415-442. doi: 10.1351/pac200476020415
- HOSSNER, L. R., MING, D. W., HENNINGER, D. L. and ALLEN, E. R. (1991): Lunar outpost agriculture. *Endeavour*, 15(2): 79-85. doi: 10.1016/S0160-9327(05)80009-2
- KOŠLER, J., MAGNA, T., MLČOCH, B., MIXA, P., NÝVLT, D. and HOLUB, F. V. (2009): Combined Sr, Nd, Pb and Li isotope geochemistry of alkaline lavas from northern James Ross Island (Antarctic Peninsula) and implications for back-arc magma formation. *Chemical Geology*, 258(3–4): 207-218. doi: 10.1016/j.chemgeo.2008.10.018
- LE MAITRE, R. W., STRECKEISEN, A., ZANETTIN, B., LE BAS, M. J., BONIN, B. and BATEMAN, P. (Eds.) (2002): Igneous rocks: A classification and glossary of terms: Recommendations of the international union of geological sciences subcommission on the systematics of igneous rocks. Cambridge University Press, Cambridge (2nd ed.), 256 p.
- KUBOVÁ, J., STREŠKO, V., BUJDOŠ, B., MATUŠ, P. and MEDVEĎ, J. (2004): Fractionation of various elements in CRMs and in polluted soils. *Analytical and Bioanalytical Chemistry*, 379(1): 108-114. doi: 10.1007/s00216-004-2612-4
- MING, D. W., HENNINGER, D. L. (1994): Use of lunar regolith as a substrate for plant growth. *Advances in Space Research*, 14(11): 435-443. doi: 10.1016/0273-1177(94)90333-6
- MLČOCH, B., NÝVLT, D. (2013): Vulkanismus a zalednění prostoru ostrova Jamese Rosse. In: P. Prošek (ed.): Antarktida. Academia Press, pp. 253–264.
- MLČOCH, B., NÝVLT, D. and MIXA, P. (Eds.) (2018): Geological map of James Ross Island – Northern part 1:25,000. Czech Geological Survey, Prague, Czech Republic.
- MORTLEY, D. G., AGLAN, H., BONSI, C. K. and HILL, W. A. (2000): Growth of sweetpotato in lunar and Mars simulants. SAE Technical Paper, 2000-01-2289. doi: 10.4271/2000-01-2289

- NARENDRANATH, S., PILLAI, N.S., TADEPALLI, S. P., SARANTOS, M., VADODARIYA, K., SARWADE, A., RADHAKRISHNA V, and TYAGI, A. (2022): Sodium distribution on the Moon. *The Astrophysical Journal Letters*, 937(2): L23. doi: 10.3847/2041-8213/ac8d7f
- PAUL, A.-L., ELARDO, S. M. and FERL, R. (2022): Plants grown in Apollo lunar regolith present stress-associated transcriptomes that inform prospects for lunar exploration. *Communications Biology*, 5(1): 382. doi: 10.1038/s42003-022-03372-4
- RAURET, G., LÓPEZ-SÁNCHEZ, J. F., SAHUQUILLO, A., BARAHONA, E., LACHICA, M., URE, A. M., DAVIDSON, C. M., GOMEZ, A., LÜCK, D., BACON, J., YLI-HALLA, M., MUNTAUB, H. and QUEVAUVILLER, PH. (2000): Application of a modified BCR sequential extraction (three-step) procedure for the determination of extractable trace metal contents in a sewage sludge amended soil reference material (CRM 483). *Journal of Environmental Monitoring*, 2(3): 228-233. doi: 10.1039/B001496F
- SCHRADER, C., RICKMAN, D., MCLEMORE, C., FIKES, J., STOESER, D., WENTWORTH, S. and MCKAY, D. (2009): Lunar regolith characterization for simulant design and evaluation using figure of merit algorithms. *In: 47th AIAA Aerospace Sciences Meeting including The New Horizons Forum and Aerospace Exposition*, 755 p.
- SMELLIE, J. L., JOHNSON, J. S., MCINTOSH, W. C., ESSER, R., GUDMUNDSSON, M. T., HAMBREY, M. J. and VAN WYK DE VRIES, B. (2008): Six million years of glacial history recorded in volcanic lithofacies of the James Ross Island Volcanic Group, Antarctic Peninsula. *Palaeogeography, Palaeoclimatology, Palaeoecology*, 260(1–2): 122-148. doi: 10.1016/j.palaeo.2007.08.020
- SMELLIE, J. L., JOHNSON, J. S. and NELSON, A. E. (2013): Geological map of James Ross Island. I. James Ross Island Volcanic Group (1:125,000 Scale). BAS GEOMAP 2 Series, Sheet 5, British Antarctic Survey, Cambridge.
- SMELLIE, J. L., MCARTHUR, J. M., MCINTOSH, W. C. and ESSER, R. (2006): Late Neogene interglacial events in the James Ross Island region, Northern Antarctic Peninsula, dated by Ar/Ar and Sr-isotope stratigraphy. *Palaeogeography, Palaeoclimatology, Palaeoecology*, 242(1–2): 169-187. doi: 10.1016/j.palaeo.2006.05.020
- STAVRAKAKIS, H.-A., ARGYROU, D. and CHATZITHEODORIDIS, E. (2022): Introducing the first Greek Martian and Lunar Simulants. Europlanet Science Congress 2022, Granada, Spain, 18–23 September 2022, EPSC2022-611. doi: 10.5194/epsc2022-611
- STEENSTRA, E. S., AGMON, N., BERNDT, J., KLEMME, S., MATVEEV, S. and VAN WESTRENNEN, W. (2018): Depletion of potassium and sodium in mantles of Mars, Moon and Vesta by core formation. *Scientific Reports*, 8: 7053. doi: 10.1038/s41598-018-25505-6
- URE, A. M., QUEVAUVILLER, PH., MUNTAUB, H. and GRIEPINK, B. (1993): Speciation of heavy metals in soils and sediments. An account of the improvement and harmonization of extraction techniques undertaken under the auspices of the BCR of the Commission of the European Communities. *International Journal of Environmental Analytical Chemistry*, 51(1–4): 135-151. doi: 10.1080/03067319308027619